*Materials Science-Poland*, *Vol. 28*, *No. 4*, *2010*

# Room temperature ferromagnetism in Si nanocaps on self-assembled glass beads

Y.C. CHI[1]*, Y. LIOU[2]

[1]Institute of Materials Engineering, National Taiwan Ocean University, Keelung, 20224 Taiwan, Republic of China

[2]Institute of Physics, Academia Sinica, Taipei, 11529 Taiwan, Republic of China

Based on self-assembly techniques, Si layers of various thicknesses were deposited on glass bead arrays of various dimensions. The experimental results support the view that the self-assembled glass beads of small sizes (i.e., 10 and 20 nm in diameter), covered with a Si layer below 5 nm in thickness, can induce ferromagnetism. Regularity in the saturation magnetization confirms that the ferromagnetic-like behaviours heavily depend on both the size of the glass beads as well as the thickness of Si nanocaps. Maximum magnetization (750 emu/cm$^3$) was found in the 20 nm glass bead template on which was deposited an ultra-thin 1 nm Si layer. We suggest that the quantum confinement mechanism helps to promote the unpaired electrons, which interact with neighbouring counterparts through the tunnelling effect and, thus, contribute to room temperature ferromagnetism.

Keywords: *ferromagnetism; nanosphere lithography; quantum confinement; exciton Bohr radius; tunnelling effects*

## 1. Introduction

Ferromagnetism is one of the most important quantum-mechanical phenomena in atomic systems. Only atoms with partially filled shells (i.e., unpaired spins) can experience a net magnetic moment in the absence of an external field. However, in recent years, many developments in systems such as $CaB_6$ [1], $HfO_2$ [2], or special forms of carbon [3] have been reported as having magnetic order above room temperature. Moreover, efforts have concentrated on studying the onset of the nanoscale systems. The reduced sizes and dimensions of certain materials have given rise to a renewed scientific interest in producing magnetism in systems that are originally nonmagnetic in their bulk state [4–7]. Quantum magnetism has become one of the most challenging areas of condensed matter and materials physics. More recently, Gari-

*Corresponding author, e-mail: chiyc@aec.gov.tw

taonandia et al. reported that nanoparticles of Au, Ag, and Cu of the size of 2 nm can exhibit magnetic behaviour at ambient temperature [8]. Liou et al. reported inspiring ferromagnetic findings in Ge quantum dots (QDs) [9, 10]. Those studies demonstrate the existence of ferromagnetism without the contribution of magnetic transition metals. In addition, theories such as that of Lieb and Kagome, have been introduced in order to predict the possibilities of flat-band ferromagnetism in quantum dot arrays [11–14]. However, even though many investigations on the general physical properties of Si have been extensively reported, no ferromagnetism has ever been ascribed to Si, due to its intrinsic behaviour and bulk structures, leaving the study of silicon as the last virgin territory of research into magnetism, and which still needs to be fully explored.

The discovery of room-temperature visible photoluminescence in Si has been confirmed [15, 16]. The size dependence of the energy gap of Si nanostructures has also been discussed extensively [17–19]. The quantum confinement effect, resulting in a blue shift of the energy gap with decreasing size, is widely believed to be responsible for the novel properties. This strongly implies that when Si has the form of low-dimensional structures such as Si QDs, its physical properties are quite different from those of its bulk state. Furthermore, Ren et al. show that a Si cluster of 4.9 nm in diameter has virtually the same band gap and density of states as a bulk Si crystal [20]. Recently, Yamamoto et al. observed that Si clusters in $SiO_2$ glass film matrices with average diameters of 3, 4, and 5.1 nm exhibit quantum confinement effects [21]. Moreover, Si has an exciton Bohr radius ($a_\beta$) of 4.9 nm [22], thus, if nanoscale Si can be involved in the formation of ordered magnetic states beneath the dimension of ca. 5 nm, it will become one of the most promising directions for magnetism research.

One simple self-assembly approach, i.e. nanosphere lithography, is introduced to control the placement of the Si layers on top of the nanospheres. This technique is an effective method of growing large area and well ordered arrays. With the aid of nanosphere lithography, a closely-packed, hexagonal array can be easily formed, in which triangular voids exist among any three nanospheres that are in physical contact with each other. When a Si layer is deposited on the substrate, many hemispherical Si nanocaps which nicely mimic the shapes of the nanospheres underneath are expected to form due to the masking effect. Part of the Si flux may penetrate through the voids and accumulate on the surface of the underlying substrate. It is worth noting that the masking effect normally decreases with the size of the nanospheres, thus the evaporated Si flux cannot easily pass through the increasingly ultrasmall triangular voids. As a result, the Si flux would seal off the voids and, further, coalescence to form a continuous film on top of the template.

## 2. Experimental

In this experiment, glass beads of four sizes (i.e., 10, 20, 50, and 100 nm in diameters) are obtained, which were diluted in a solution of surfactant Triton (Aldrich) and

well-mixed with isopropanol (1:1000 for small glass beads and 1:600 for large glass beads; ratio by volume). To make contaminant-free samples, the clearing procedure is strictly observed. Si substrates ($7\times7\times0.5$ mm$^3$) are first cleaned by the Piranha method. This cleaning process can remove organic and certain metal contaminants, and result in a hydrophilic surface. To degrease the surface of the substrate, solvent-based cleaning, with sequences of acetone, methanol and deionized water were used, each sonicated for 30 min. Solution was dipped and then spin-coated on Si substrate below 500 rpm (Chemat Tech., KW-4 A). High-purity intrinsic Si (99.9999%) is obtained as the deposition source. Si layers of various thicknesses (i.e., 1, 2, 3, 5, and 10 nm) were chosen to carry out thermal deposition onto various glass bead templates. A low deposition rate (0.1 nm/min) was selected during the evaporation process, which was performed under the pressures of $1\times10^{-7}$ Torr. Energy dispersive spectroscopy (EDS) was used to investigate the impurities. Within the detection limit (0.1%) of EDS, neither intact Si targets (bulk form) nor deposited samples (layer form) indicate the presence of magnetic contaminants. The magnetization measurements of the samples were carried out by using a vibrating sample magnetometer (VSM) at room temperature. Both atomic force microscopy (AFM) and field emission scanning electron microscopy (FESEM) were chosen to investigate the morphological evolutions of the Si samples.

## 3. Results and discussion

Based on the above, a scheme is proposed: self-assembled glass beads covered with Si layers of various thicknesses are introduced, as schematically shown in Fig. 1a. If the

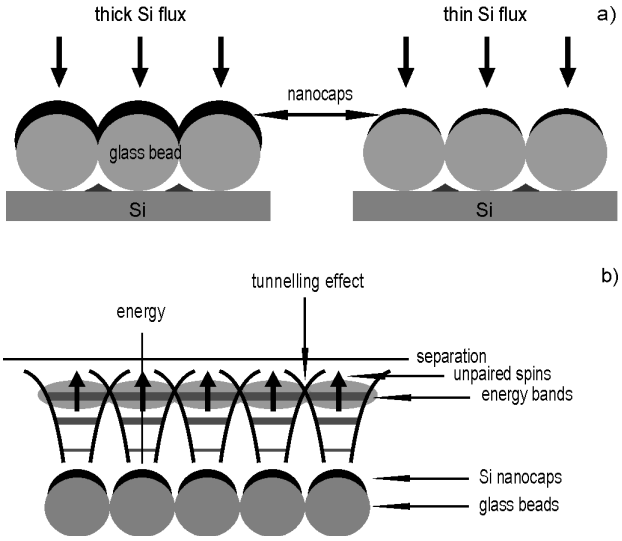


Fig. 1. An illustrative scheme of Si deposition characterized by thick and thin fluxes onto a glass bead arrays (a) and a simplified scheme introducing an ideal nano-scale ferromagnetic system of Si (b)

deposited Si layer is thick enough, all forms of the glass beads will be wrapped by Si. In this case, good hysteresis loops are not expected to occur, because a substantial quantity of Si in the initial deposition layer becomes transferred to the film. On the other hand, for light deposition, appropriate hemispherical nanocaps are expected to form. We suggest that when the Si nanocaps are sufficiently small, degenerated energy levels split into discrete levels as a consequence of the quantum confinement effects. At such ultra-small dimensions, unpaired spins are likely to contribute to the magnetic moments, which interact with neighbouring counterparts through the tunnelling effect and then initiate the quantum ferromagnetism. However, in the extreme case (i.e., the 10 nm glass bead array), we recall that if the voids are too small, they may extensively block the penetration of the Si flux, due to the fading of the masking effect. Many enlarged nanocaps are expected to form all over the template and effectively degrade ferromagnetism. Therefore, on the contrary, they may not necessarily show the largest magnetizations. Yet on top of the large glass beads (e.g., 100 nm in diameter), thin but larger nanocaps are not expected to display strong ferromagnetism either, for both the enlarged nanocaps (far beyond $a_\beta$) and the voids may seriously impair the quantum confinement effects. In Figure 1b, a schematic diagram illustrates the discrete energy bands that are involved, confined energy barriers, unpaired spins, and so forth, in an ideal nanoscale Si system (i.e., a template comprised of small uniform glass beads and thin Si nanocaps).

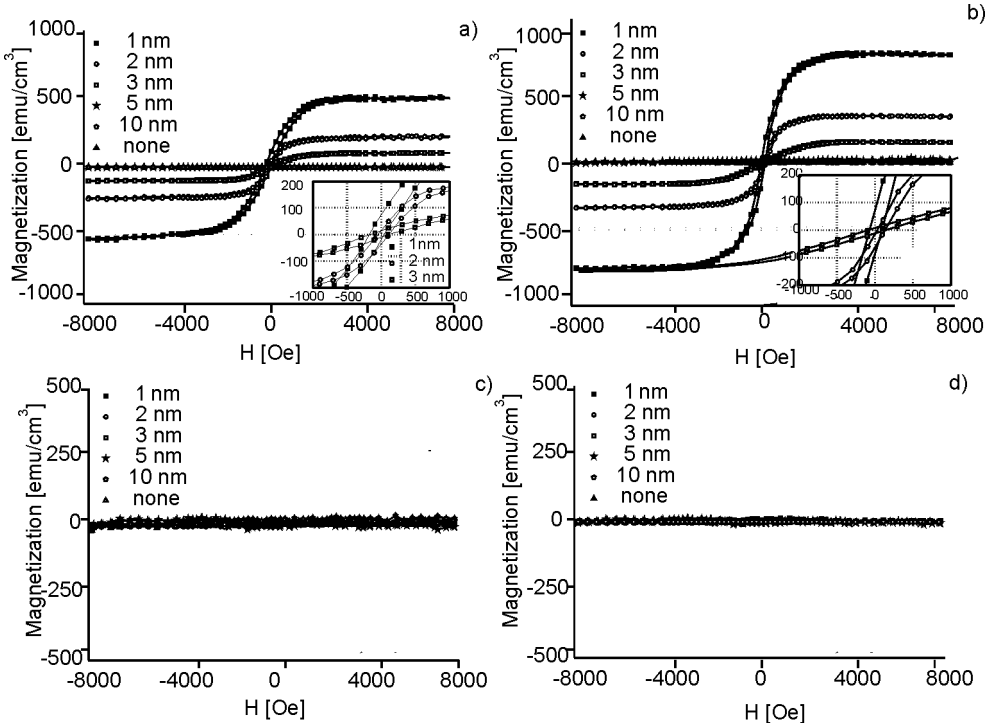


Fig. 2. Room temperature magnetization loops (per unit volume) vs. external magnetic field of: a) 10 nm, b) 20 nm, c) 50 nm, and d) 100 nm glass bead arrays deposited with various Si layers

Figure 2 shows the room temperature magnetization loops (per unit volume) vs. the external magnetic fields of the samples (i.e., 10, 20, 50, and 100 nm glass bead arrays deposited with various Si layers) without the diamagnetic contribution of the substrate. We find that in Figs. 2a, b, the 10 nm and 20 nm glass bead templates deposited with various Si layers show ferromagnetic hysteresis loops with amazing regularities. As the deposited Si layer increases from 1 to 5 nm, the saturation magnetization consistently decreases from the maximum value down to null. The highest magnetization (~750 emu/cm$^3$) was found in the 20 nm glass bead array on which was deposited an ultra-thin 1 nm Si layer. The insets show the magnification of the hysteresis loops of the 10 nm and 20 nm templates, each of which were deposited, at low field strength, with 1, 2, and 3 nm Si layers. However, if the glass bead arrays are large (i.e., 50 nm or 100 nm in diameter), then diamagnetism always occurs, regardless of the thickness of the Si layer deposited on the surfaces of the beads, as shown in Figs. 2c,d. We found no significant magnetic signals with such samples.

For a clear description, we take two representative arrays, i.e. 20 nm and 100 nm glass bead arrays. Si layers of various thicknesses were deposited on each of these types of arrays to illustrate the comparative performance in ferromagnetism. The former type of array is selected for its better quantum confinement mechanism in magnetic presentations, whereas the latter is chosen because its dimension is far greater than $a_\beta$ and because it exhibits the worst magnetization. By using FESEM, we carefully investigate the morphological evolutions of the samples. In Figure 3a, which shows the micrograph of a 20 nm bead array deposited with 1 nm Si, we can directly observe that these nanocaps, lying on top of the glass beads, have good shapes. When these nanocaps are close enough to each other, room temperature ferromagnetism occurs. However, due to weak communications (i.e., tunnelling effects) among these unpaired spins, the squareness of the hysteresis loop cannot be broadened dramatically. In Figure 3b, the fuzzy junctions among the glass beads can barely be observed for 2 nm Si coverings upon the template. The magnetization was found to be reduced to 300 emu/cm$^3$. Yet as the thickness of the Si layer increases to 3 nm, apparent junctions emerged in the vicinity of the nanocaps, as shown in Fig. 3c. Correspondingly, poor magnetization (ca. 140 emu/cm$^3$) arises at this stage, which implies that the presence of homogeneous Si junctions does not enhance ferromagnetism, but spoils it. In Figure 3d, when the Si layer increases to 5 nm, we can see a clear continuous film formed on top of the template. The magnetization undoubtedly drops to null. Similarly, in Fig. 3e, when the Si layer increases to 10 nm, we get the same diamagnetic result as that which occurs with the 5 nm Si layer. No hysteresis loops can be detected, just as expected. The drops in the saturation magnetizations basically comply with the increasing thickness of the nanocaps, for layer thicknesses below 5 nm. Once the nanocaps thicken to 5 nm or above, they immediately lose all their ferromagnetism.

For the largest glass bead arrays (i.e., 100 nm in diameter), Figs. 3f, g show the micrographs, barely visible, of the 1 nm and 2 nm Si nanocaps on top of the templates, respectively. Likewise, as the thickness increases to 3 nm, fuzzy junctions with

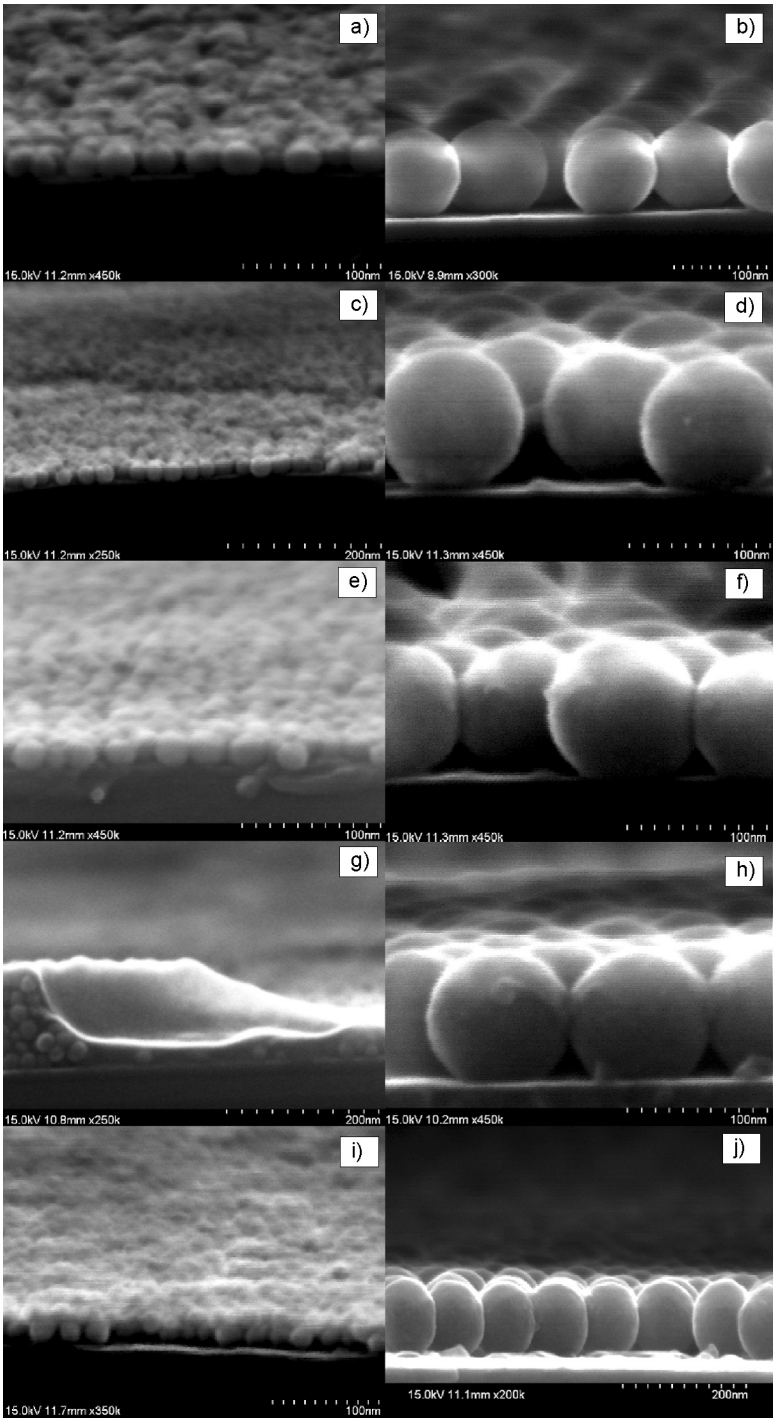


Fig. 3. Cross-sectional FESEM micrographs of various Si layers on 20 nm glass bead arrays (a)–(e), and on 100 nm glass bead arrays (f)–(j)

nanocaps gradually appear, as shown in Fig. 3h. For thicker depositions (i.e., 5 nm and above), Figs. 3i, j illustrate the tendency of the Si flux to form coalescent nanocaps on the templates. Unfortunately, they are all diamagnetic. None of them exhibit the slightest ferromagnetism, due to thick coverings (thicknesses far greater than $a_\beta$) on the beads and the prevalence of large voids on the substrate. They dynamically prevent the moment coupling, leading to null magnetism. Therefore, neither 1 nor 10 nm layers of Si deposited on the 100 nm glass bead arrays result in measurable magnetism.

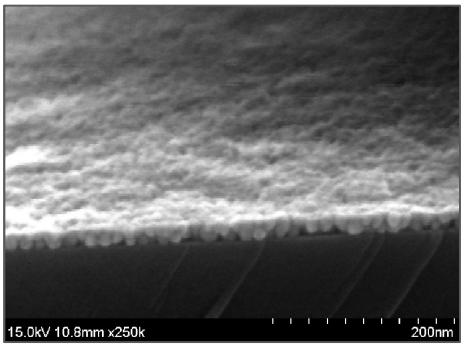


Fig. 4. Cross-sectional FESEM micrograph of 1 nm Si deposited on top of a 10 nm glass bead array

Initially, we expect to observe stronger magnetism in the 10 nm glass bead array deposited with thin nanocaps than that of its counterpart, i.e. the 20 nm glass bead array. But this does not happen at all. Upon re-examining the samples, we find that the 10 nm glass bead array deposited with a 1 nm Si layer suffers a coalescence problem, as shown in Fig. 4. Ties and junctions can be clearly seen on top of the beads. The fading of the masking effect helps in the formation of larger nanocaps, resulting in extensive magnetic degradation. On the other hand, the 20 nm glass bead template can induce the formation of many isolated, uniformly-distributed nanocaps. We hardly see any serious coalescence in the latter case, unless a thick Si layer redistributes itself. We speculate that if the voids are a suitable size, this will help Si flux to penetrate through without detrimental seal-off. Therefore, the magnetizations of the 10 nm glass bead arrays, whether they are deposited with 1, 2, or 3 nm thick layers of Si, are always inferior to those of the 20 nm glass bead arrays.

In view of the fact that the thin 1 nm Si nanocaps on the 20 nm glass bead array result in the largest saturation magnetization, we therefore claim that Si nanocaps can exhibit room temperature ferromagnetism provided that the optimum glass beads, with appropriately thin Si coverings, are in mutual contact. However, if the size of the glass beads increases above 50 nm and/or if the Si layer thickens above 5 nm, the magnetization quickly decreases to background levels (diamagnetism). This can be attributed to the following causes. Firstly, the dimension of the thin nanocaps having Si deposition layers of 1 or 2 nm thick, and lying on top of the 50 nm (or 100 nm) glass beads, far exceeds the quantum confinement edge (ca. 5 nm). Moreover, the long centre-to-centre distance of the beads and the prevalence of the large voids prohibit the occurrence of the exchange interactions, thereby leading to the smallest level of magnetization.

Secondly, a thick layer (e.g., 5 nm or 10 nm) deposited on any template will eventually transform into continuous film. A 5 nm thick Si layer is too thick to form isolated, quantum-sized nanocaps on top of the beads, regardless of the bead size (see Figs. 3d, i). AFM micrographs support this finding, as shown in Fig. 5. Significant coalescence (i.e., 5 nm Si) can be clearly observed on both the 20 nm glass bead array (Fig. 5a) as well as on the 100 nm glass bead array (Fig. 5b). This implies that thick Si layers always induce the least, or negligible, ferromagnetism. We suggest that the missing quantum confinement effects are responsible for the great loss of the induced ferromagnetism.

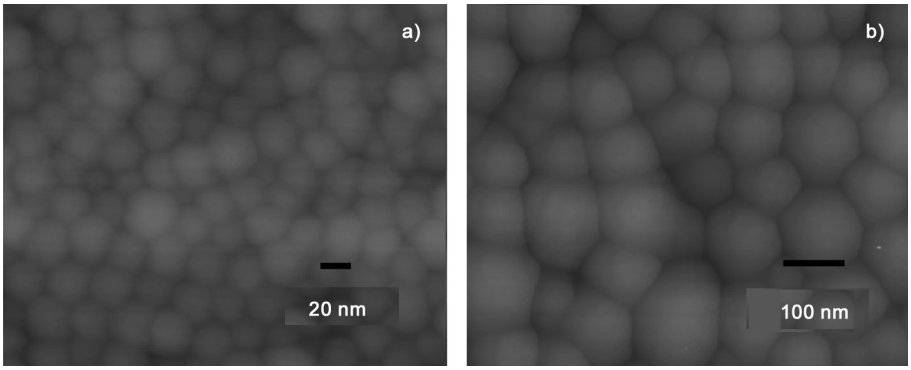


Fig. 5. AFM micrographs of (a) the 20 nm glass bead array and (b) the 100 nm glass bead array deposited with 5 nm Si, respectively

Magnetic impurities are always present, even though considerable precautions have been taken to preclude contaminants that might contribute to magnetic interference. However, impurities can be ruled out by considering the following facts: (1) the evidence of EDS examinations; (2) theoretical assessment [9]. For example, if there were a large amount of magnetic impurities of ca. 500 ppm (0.05%) in the samples, the maximum saturation magnetization per unit volume would be expected to be ca. 0.5 emu/cm$^3$, which is much smaller than the actual magnetization measurements of this study; (3) linear increment of the thickness of Si layer accompanies a corresponding decrement in the saturation magnetization. If significant magnetic impurities had been present, we would have measured ascending levels of magnetization corresponding to the increment in the layer thickness; and (4) all magnetic samples exhibited a spontaneous and continuous decay in magnetization strength when they were left to stand alone for a period of time. However, magnetic contaminants should maintain stable magnetism on the host material, unless an effective purge was carried out.

## 4. Conclusions

Based on self-assembly techniques, glass bead arrays deposited with Si layers of various thicknesses (i.e., 1–10 nm) were investigated. The 10 nm and 20 nm glass bead arrays having Si deposition layers of various thicknesses induce ferromagnetic hysteresis loops with remarkable regularities. Maximum magnetization (ca. 750 emu/cm$^3$)

was found in the 20 nm glass bead array deposited with an ultrathin 1 nm Si layer. Regularity in saturation magnetizations confirms that the ferromagnetic-like Si nanocaps heavily depend on both the size of the glass beads as well as on the thickness of the Si layers. Quantum confinement on excitons in variously sized Si nanocaps has been proposed as the most reasonable explanation for the quantum ferromagnetism. The experimental results support the view that the quantum confinement mechanism helps to promote unpaired electrons which interact with neighbouring counterparts through the tunnelling effect, and then initiate the quantum ferromagnetism. However, the squareness of the hysteresis loops cannot be arbitrarily broadened, due to weak interactions among these unpaired spins.

In this study, we provided evidence for soft ferromagnetic behaviour in Si nanocaps at room temperature. It has been suggested that very small Si nanocaps exhibit a localized magnetism, in contrast to the diamagnetism characteristic of bulk Si. The possibility of controlling the magnetization might open up a wide area of research on quantum ferromagnetism. Ferromagnetic nano-scale Si systems might possibly be utilized and exploited.

**Acknowledgements**

This research has been partially supported by the Atomic Energy Council of Taiwan. The author acknowledges S.T. Chiou (ROCAEC), Y.M. Lan, C.L. Chen, C.S. Tsai and T.W. Chu (INER) for their expert support.

## References

[1] DORNELES L.S., VENKATESAN M., MOLINER M., LUNNEY J.G., COEY J.M.D., Appl. Phys. Lett., 85 (2004), 6377.
[2] COEY J.M.D., VENKATESAN M., STAMENOV P., FITZGERALD C.B., DORNELES L.S., Phys. Rev. B, 72 (2005), 024450.
[3] ESQUINAZI P., HÖHNE R., J. Magn. Magn. Mater., 290 (2005), 20.
[4] HERNANDO A., SAMPEDRO B., LITRÁN R., ROJAS T.C., SÁNCHEZ-LÓPEZ J.C., FERNÁNDEZ A., Nanotechnology, 17 (2006), 1449.
[5] DUTTA P., PAL S., SEEHRA M.S., ANAND M., ROBERTS C.B., Appl. Phys. Lett., 90 (2007), 213102.
[6] WANG W.C., KONG Y., HE X., LIU B., Appl. Phys. Lett., 89 (2006), 262511.
[7] SUBER L., FIORANI D., SCAVIA G., IMPERATORI P., PLUNKETT W.R., Chem. Mater., 19 (2007), 1509.
[8] GARITAONANDIA J.S., INSAUSTI M., GOIKOLEA E., SUZUKI M., CASHION J.D., KAWAMURA N., OHSAWA H., DE MURO I.G., SUZUKI K., PLAZAOLA F., ROJO T., Nano Lett., 8 (2008), 661.
[9] LIOU Y., SHEN Y.L., Adv. Mater., 20 (2008), 779.
[10] LIOU Y., SU P.W., SHEN Y.L., Appl. Phys. Lett., 90 (2007), 182508.
[11] MIELKE A., J. Phys. A, 24 (1991), L73.
[12] LIEB E.H., Phys. Rev. Lett., 62 (1989), 1201.
[13] TASAKI H., Phys. Rev. Lett., 69 (1992), 1608.
[14] MOULTON B., LU J.J., HAJNDL R., HARIHARAN S., ZAWOROTKO M.J., Angew. Chem. Int. Ed., 41 (2002), 2821.
[15] TAKAGI H., OGAWA H., YAMAZAKI T., ISHIZAKI A., NAKAGIRI T., Appl. Phys. Lett., 56 (1990), 2379.
[16] CANHAM L.T., Appl. Phys. Lett., 57 (1990), 1046.
[17] WANG L.W., ZUNGER A., J. Phys. Chem., 98 (1994), 2158.

[18] YORIKAWA H., UCHIDA H., MURAMATSU S., J. Appl. Phys., 79 (1996), 3619.
[19] KUX A., CHORIN M.B., Phys. Rev. B, 51 (1995), 17535.
[20] REN S.Y., DOW J.D., Phys. Rev. B, 45 (1992), 6492.
[21] YAMAMOTO M., HAYASHI R., TSUNETOMO K., KOHNO K., OSAKA Y., Jpn. J. Appl. Phys., 30 (1991), 136.
[22] CULLIS A.G., CANHAM L.T., CALCOTT P.D.J., J. Appl. Phys., 82 (1997), 909.

*Received 20 June 2010*